

pubs.acs.org/Macromolecules Article

Adsorption of Charge Sequence-Specific Polydisperse **Polyelectrolytes**

Vaidyanathan Sethuraman, David Zheng, David C. Morse, and Kevin D. Dorfman*



Cite This: Macromolecules 2022, 55, 3030-3038



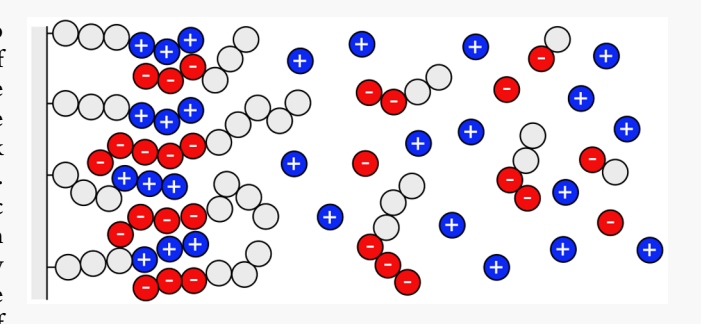
ACCESS I

Metrics & More

Article Recommendations

Supporting Information

ABSTRACT: We use coarse-grained molecular dynamics to elucidate the influence of polydispersity on the adsorption of polydisperse bulk polyanionic chains onto a monodisperse polycationic brush. We consider primarily two different charge sequence scenarios, in which both polymer species are either block and alternating, for polyanions with a fixed dispersity D = 1.5. Polydispersity plays a negligible role when the brush cationic chains are in excess, since all polyanionic chains are adsorbed. In contrast, when the polyanions are in excess, polydispersity substantially decreases the fraction of chains adsorbed into the brush, irrespective of charge sequence, but increases the number of



monomers adsorbed. These opposing trends are made possible by selective adsorption of long chains.

INTRODUCTION

Oppositely charged polyelectrolytes aggregate owing to, at first approximation, the entropy gain from counterion release when two oppositely charged polyelectrolytes charge neutralize one another. In a salt solution, this process is sometimes termed complex coacervation, wherein a liquid-liquid phase separation produces a polymer rich (coacervate) phase and a polymer lean (supernatant) phase. 1-5 Coacervation plays an important role, for example, in the formation of proteinpolyelectrolyte complexes. 6-11 Another important case of polyelectrolyte aggregation is the adsorption of polyelectrolytes to oppositely charged polyelectrolytes with limited mobility, for example, in layer-by-layer assembly on a surface 9,12-16 or adsorption onto a micelle corona. 17,18

A particularly intriguing question is whether the location of the charges along the polyelectrolyte, i.e., the charge sequence, plays a role in the adsorption phenomena. Using both experiments and simulations, Perry, Sing, and co-workers showed that polyelectrolyte complexation in solution can be engineered by tuning the charge sequence on the polymer backbone alone in polyelectrolyte-salt systems. 19 We have been interested in understanding whether their results for polyelectrolyte solutions extend to the companion problem of polyelectrolyte adsorption using a surface-mobile polymer brush as a tractable model for mimicking the micelle adsorption problem. Our previous simulations showed that the equilibrium properties of adsorbed monodisperse polyelectrolytes are charge-sequence-dependent, 21 in a manner qualitatively consistent with the corresponding observation for complex coacervation in solution. 19

An open issue regarding polyelectrolyte complexation, either in solution or on a surface, is whether the sequence-

dependent phenomena observed for monodisperse systems are robust to polydispersity. Unless careful measures are taken, 22-27 polydispersity values in many polyelectrolyte solutions experiments can vary between D = 1.1 and D = 1.14.8,9,13,16 However, a systematic understanding of the role of polydispersity of the equilibrium structure of the complexes is missing, since these effects are difficult to decouple from other intrinsic properties of the system, and there appears to be no work to address this topic for adsorption to a polymer brush. Indeed, the seminal experiments used to test sequencedependent effects for coacervation were performed at low polydispersity to avoid this confounding effect. 19 Despite the polydispersity in experiments, apart from a few notable exceptions, 28,29 theory and simulations in the context of polyelectrolyte complexation are confined to monodisperse polyelectrolytes. 19,21

This work uses coarse-grained simulations to elucidate the effect of polydispersity on the adsorption efficacy of sequencespecific oppositely charged polydisperse polyelectrolytes onto a brush of monodisperse polymers. Specifically, we answer the following questions: (i) How does the polydispersity of the bulk chains affect the adsorption efficacy for a given charge sequence? (ii) Is there an effect of polydispersity on the density profile and resulting net charge within the brush? (iii) Is there

Received: December 24, 2021 March 5, 2022 Revised: Published: April 6, 2022





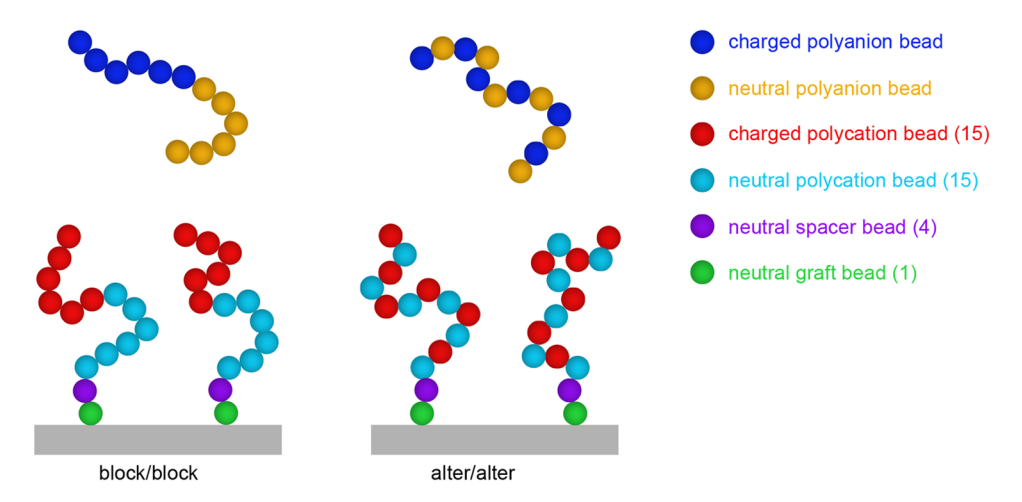


Figure 1. Schematic of the charge sequences explored in this work: block—block and alter—alter. The color-coded legends correspond to the different bead types in the polyanion and polycation chains. The numbers within the brackets of the legend indicate the number of each type of bead. The graft bead is mobile within the plane of the surface. The numbers of beads in the polyanions depend on D_{ideal} and are tabulated in Table S1.

an interplay between the charge sequence and polydispersity effects on the adsorption efficiency?

SIMULATION DETAILS

We used an implicit solvent coarse-grained molecular dynamics simulation with explicit salt and counterions, following our previous work. Without loss of generality, we consider the (initially) free chains to be polyanions and the grafted (or tethered) chains to be polycations. The number of polyanion chains $n_{\rm pa}$ was {16, 32, 64, 128, and 150}, and the number of graft chains $n_{\rm pc}$ was fixed at 32. The grafted chains contain 15 charged beads and 15 uncharged beads, with the surface linker comprising a single neutral graft bead and four neutral spacer beads to avoid surface artifacts. 21

The degree of polymerization for polyanions was drawn from a Schulz–Zimm distribution 30,31 with a target polydispersity value $D_{\rm ideal}$ and a number-average degree of polymerization of N=30 to correspond to the degree of polymerization of the charge-sequence part of the monodisperse grafted chains. Owing to the small number of polymer chains in the simulations, the polydispersity $D_{\rm sim}$ realized in a given simulation is somewhat different from $D_{\rm ideal}$. The error criterion and the different constraints imposed in generating the initial structure are described in section S1 of the Supporting Information. The PDI values and number of monomers of each type for all the cases simulated are tabulated in the Supporting Information (Table S1).

We chose the two different sets of charge sequences in Figure 1 as the primary focus of our work. For consistency, we follow the naming conventions in our previous work: ²¹ (i) "block—block" corresponds to a system wherein the charge sequence of polycation brush and the polyanions form a block charge sequence architecture, and (ii) "alter—alter" corresponds to a system wherein the charge sequence of the tethered polycations and the polyanions form an alternating charge sequence architecture. We will briefly discuss a limited set of additional results for the block—alter and alter—block cases at the end of our discourse.

Simulations were performed in an NVT ensemble by using the LAMMPS software.³² The model parameters used in this work are somewhat different than our prior work²¹ (see section

S1 in the Supporting Information). For this reason, we have simulated both the monodisperse case $\mathcal{D}=1.0$ and the polydisperse case $\mathcal{D}=1.5$ here. A detailed description of the system setup and the measures used to quantify the results can be found in our previous work²¹ and, briefly, in the Supporting Information, section S1. Reported results are averaged from four independent simulations, where each simulation draws its own distribution of N for the polyanion chains from the Schulz–Zimm distribution.

To quantify the number of bound polyanion chains, we consider an untethered *chain* to be bound to the brush region if least one the monomers (charged or neutral) of the bulk polyanion chain is within a cutoff distance (r_c) of *any* polycation brush monomer.²¹ To quantify the number of bound *monomers* of the polyanion chains, we simply sum the monomers of each bound polyanion chain. For both of these calculations, we exclude the neutral spacer beads connecting the charged monomers to the grafted surface and the grafted bead of the brush chains for this calculation. We choose a cutoff $r_c = 1.50\sigma$ that is slightly larger than the range of the pair interaction.

RESULTS

The first key insight from simulations of polydisperse polyanions is that polydispersity has a very small effect on the overall density profile of the anionic monomers and graft monomers within the brush. For example, Figure 2 plots the density distributions of the polyanion (black) and polycation (green) monomers for $n_{pa}/n_{pc} = 4.7$ as a function of the distance from the grafted surface, normalized by the box length in the confined direction. Qualitatively similar results were observed for all the other values of $n_{\rm pa}/n_{\rm pc}$ simulated and reported in the Supporting Information (Figure S2). While for the block-block case (Figure 2a) there exist small differences in the density profiles of the anionic monomers near the edge of the brush $(z/L_z \approx 0.22)$ between the monodisperse and polydisperse cases, the density profiles of the grafted and anionic monomers for the alter-alter cases (Figure 2b) are practically indistinguishable between the monodisperse and polydisperse systems.

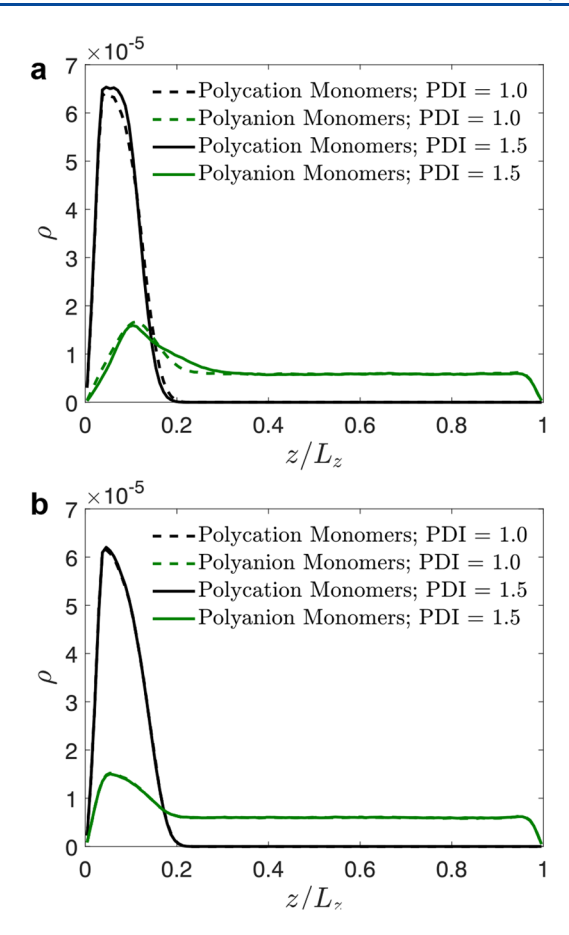
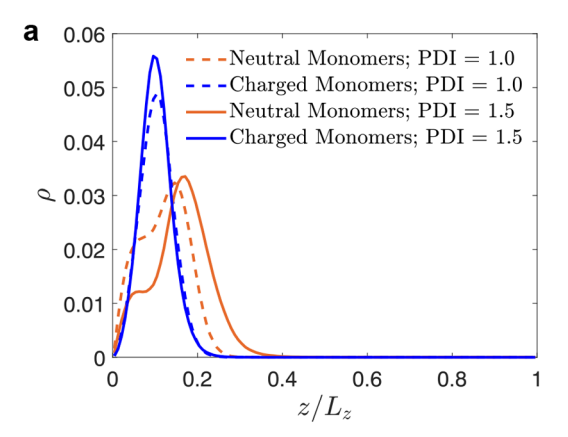


Figure 2. Density profiles for the grafted polycation and polyanion monomers for the (a) block—block and (b) alter—alter architecture for $n_{\rm pa}/n_{\rm pc}=4.7$, as a function of the distance from the grafted surface z, normalized by the box length in the confined direction L_z . The spacer blocks are not included for the polycation chain. The density profiles for other cases are plotted in Figure S2. The spacer and neutral beads are excluded while computing the densities of the grafted polymers.

The interpretation of Figure 2 is relatively straightforward. Starting from an initial condition where the charges on polyelectrolytes within the brush are neutralized by counterions, the entropic gain from counterion release from the brush drives the adsorption of polyelectrolytes into the brush. The process is somewhat more complicated than this simple picture because of overcharging of the brush,³³ as we discussed elsewhere for the monodisperse case.²¹ Nevertheless, the key conclusion is that polydispersity appears to have a small effect on these processes; chains adsorb into the brush to create approximately the same monomer density profile for both the monodisperse and polydisperse cases. In addition, the radius of gyration of the grafts becomes smaller (Figure S3) when polyanion chains are adsorbed onto the grafts because of the increased screening. However, the reduction in the radius of gyration of grafts is independent of polydispersity.

While the overall monomer density profiles are relatively insensitive to polydispersity, the situation is somewhat different for the distribution of monomers corresponding solely to the adsorbed polyanions. For the block—block system, the preferred configuration of the adsorbed chains is to insert their charged block into the brush, with the neutral tail remaining outside the brush to increase the configurational entropy. Figure 3a demonstrates that in the polydisperse



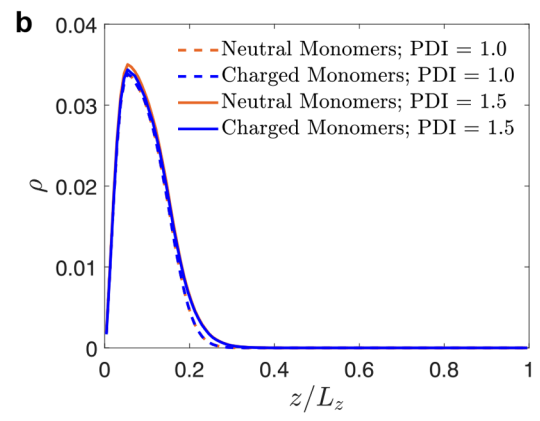


Figure 3. Density profiles for the neutral and charged monomers for adsorbed chains for the (a) block—block and (b) alter—alter architecture for $n_{\rm pa}/n_{\rm pc}=4.7$, as a function of the distance from the grafted surface z, normalized by the box length in the confined direction L_z . The density profiles for other cases are plotted in Figure S4.

system the block—block architecture produces a longer tail of neutral monomers extending outside the brush than the monodisperse case. This effect arises due to a preference for adsorbing the longer block polyanions; the preferential adsorption of long chains and its impact will be a recurring theme throughout our discourse. In contrast, the alternating polyanions are completely adsorbed into the alternating brush. This leads to a much simpler picture; Figure 3b shows that this behavior leads to polydispersity has a relatively small effect on the monomer distribution for the alter—alter cases.

We now turn our attention to the fraction of polyanions in the system that are adsorbed onto the brush. The adsorbed fraction can be computed in two different ways. In the first method, we compute the ratio $f_{\rm ads}^{\rm mon}$ of the number of monomers that are part of a polyanion chain that is bound to the brush (i.e., to a polyanion chain for which at least one monomer is within the cutoff distance of a brush monomer) to the number of charged and neutral monomers in tethered polycations, excluding contributions of the five-monomer spacer segment of each tethered chain. This adsorbed fraction is proportional to the sum of the areas under the curves of charged and neutral bound monomers (normalized by the total number of monomers in tethered polymers excluding the spacer and grafted beads) in Figure 3 and Figure S4. We also computed the ratio fads of the number of polyanion chains that are adsorbed to the brush to the number of tethered polycation

chains. These two calculations give complementary insights into the adsorption process.

Let us consider first the fraction of polyanion monomers adsorbed to the brush, f_{ads}^{mon} . Overall, Figure 4 demonstrates

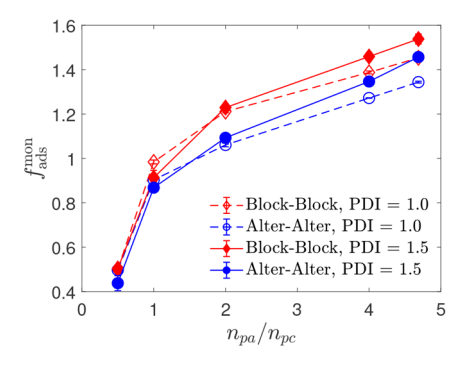


Figure 4. Adsorbed monomer ratio $f_{\text{ads}}^{\text{mon}}$ as a function of the relative ratio of polyanions to polycations for the block—block and alter—alter cases. The error bars, typically smaller than the symbol size, correspond to the standard error of the mean.

that the block—block case leads to more adsorbed monomers than the alternating case for both monodisperse and polydisperse systems. We thus infer that the thermodynamic conclusions that we drew elsewhere from simulations of the monodisperse case²¹ extend to the polydisperse system: the internal energy of adsorption favors the block—block system due to a stronger charge correlation effect.³⁴ The net effect of these trends in internal energy and entropy is a stronger adsorption of the block system, which is evident in Figure 4. When the polyanion is strongly in excess, we further observe in Figure 4 that polydispersity favors increased adsorption of monomers.

One of the most remarkable features of polyelectrolyte brushes is the ability of the brush to become overcharged in the presence of a large number of polyanions. Figure 5

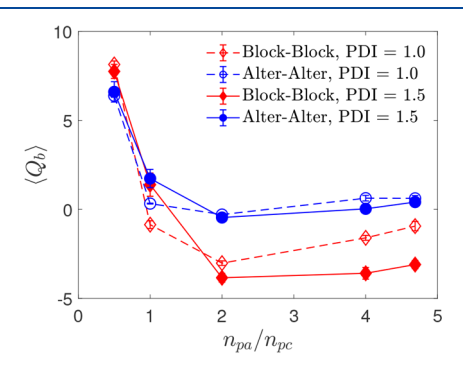


Figure 5. Total charge of the brush as a function of the ratio of polyanions to polycations. The error bars correspond to the standard error of the mean.

provides the net electrostatic charge within the brush, which includes contributions from both polyions and counterions that remain within the brush. The general trend of undercharging and then overcharging with increasing polyanion concentration is consistent with previous work. The trend of higher overcharging for the block—block system observed for the monodisperse case²¹ persists in the presence of polydispersity. For the alternating charge sequence, polydispersity provides a modest increase in overcharging that is

almost to within the error. In contrast, polydispersity leads to a statistically significant degree of additional overcharging for the block charge sequence. Overall, the trend in Figure 5 mirrors that in Figure 4.

If we instead consider adsorption efficiency in terms of the number of chains adsorbed, Figure 6 shows that the

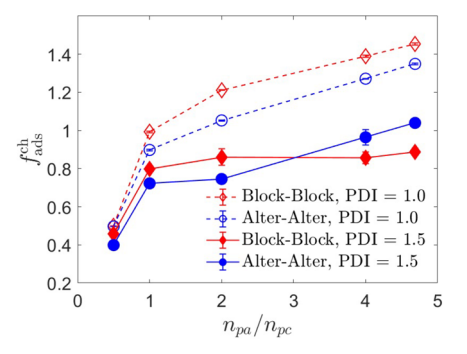


Figure 6. Fraction of adsorbed polyanions as a function of the relative ratio of polyanions to polycations for the block—block and alter—alter cases. The error bars correspond to the standard error of the mean.

phenomena appear to be more complicated. For all ratios of polyanions to polycations, Figure 6 indicates that the monodisperse case leads to more chains to adsorb to the brush than its polydisperse counterpart. The most intriguing feature of Figure 6 is the crossover in the polydisperse cases when the polyanions are in large excess, with the alternating case leading to more chains adsorbing to the brush than the block-block case, in contrast to the smaller number of monomers adsorbed for the alternating case in Figure 4. At first glance, it would seem that the larger number of adsorbed chains for the alternating case runs counter to the thermodynamic argument that favors adsorption of block sequences due to a more favorable correlation energy. 21,34 However, the calculation of the number-averaged degree of polymerization of the adsorbed chains in Figure 7 provides the resolution to this conundrum. For the block architecture, the typical degree of polymerization of the adsorbed chains exceeds those for the alternating case. As a a result, fewer chains need to be adsorbed (Figure 6) for the block-block case to achieve the requisite number of monomers adsorbed (Figure 4).

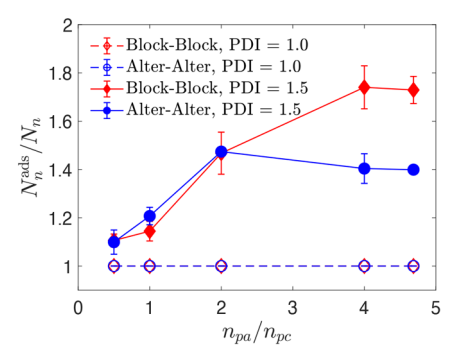


Figure 7. Ratio $N_n^{\rm ads}/N_n$ of the number-average degree of polymerization $N_n^{\rm ads}$ of adsorbed polyanion chains to the number-average degree of polymerization $N_n=30$ of all polyanion chains in the simulation, plotted vs the ratio $n_{\rm pa}/n_{\rm pc}$ of polyanions to grafted polycations for the block—block and alter—alter cases. The error bars correspond to the standard error of the mean.

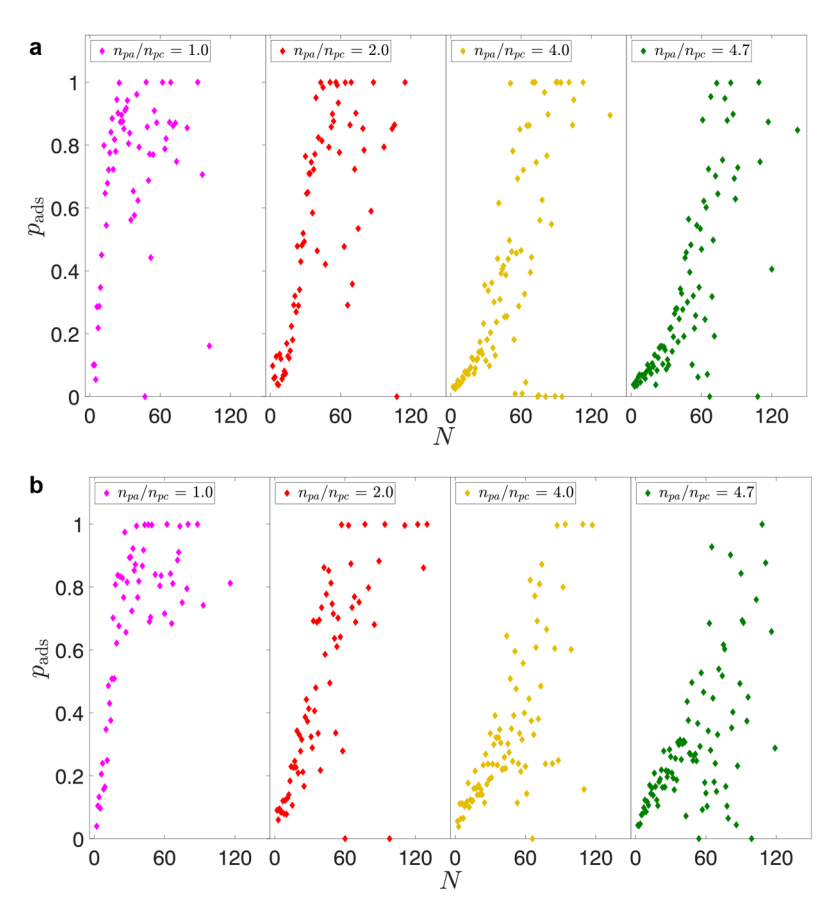


Figure 8. Probability distribution, p_{ads} , for adsorption of chains with degree of polymerization, N, for (a) block—block and (b) alternating—alternating charge sequences at different ratios of the polyanions to polycations for the polydisperse case. The charge-sequence portion of the polycation brush chains is N = 30. All the results reported were averaged across four cases.

To understand more deeply the differences between block and alternating cases exhibited in Figures 4–7, we have also computed the distribution $p_{\rm ads}(N)$ for the degree of polymerization N of bulk chains adsorbed onto the grafted chains. Figure 8 displays $p_{\rm ads}(N)$ for the block—block and alter—alter sequences for various $n_{\rm pa}/n_{\rm pc}$ for the polydisperse case. The binning in Figure 8 is done in integer values of N. For values of N near the polyanion number-averaged degree of polymerization (N=30), there can be many molecules per bin, especially as the number of polyanions increases. In contrast, for degrees of polymerization that are in the tails of the Schulz–Zimm distribution, the bin typically contains only one chain.

For all of the block—block cases in Figure 8a, $p_{\rm ads}$ for degree of polymerizations lower than the graft degree of polymerization ($N \lesssim 35$) lies mainly between 0.05 and 0.5. This suggests that the lower degree of polymerization chains exhibit a reversible adsorption—desorption kinetics during the time scale of the simulations, with many of these chains residing outside the brush. In contrast, the majority of the high degree of polymerization chains ($N \gtrsim 70$) remain adsorbed ($p_{\rm ads} = 1.0$) throughout the course of the simulation. In other words, these chains display irreversible adsorption—desorption kinetics. These trends become more apparent for $n_{\rm pa}/n_{\rm pc} = 4.0$ and $n_{\rm pa}/n_{\rm pc} = 4.7$, wherein a larger number of the high-N chains are present because there are more polyanions in the system, and this increases the likelihood of selecting a larger value of N from the Schulz—Zimm distribution. These

observations are consistent with the results of Aguilera-Granja et al.,²⁸ where they showed that the probability of adsorption of longer chains onto neutral surfaces is higher than that for the shorter chains.

The qualitative trends are similar for the block—block (Figure 8a) and alternating—alternating (Figure 8b) systems, with an increase in the probability of adsorption with increasing degree of polymerization. However, the sharpness of the increase differs between the two cases, with a slower increase for the alternating charge sequence. This behavior is consistent with the stronger adsorption of block sequences, ²¹ as illustrated previously in Figure 4.

One potentially troubling aspect of Figure 8 is the tendency for "all-or-nothing" behavior for adsorption of high degree of polymerization chains. We note two likely reasons: (i) The first is an artifact arising from the smaller number of chains of that given degree of polymerization. The Schulz-Zimm distribution function has a finitely decaying "tail" (see the theoretical Schulz-Zimm distribution function plotted in Figure S1a). Therefore, to sample highly polydisperse systems, the likelihood to sample large number of long length chains is very low unless the sample size is extremely large. For instance, for n_{pa} = 150 in Figure S1b, we can see that the number of chains with $N \approx 110 \ (100 \lesssim N \lesssim 120)$ is 2 where as the number of chains in the vicinity of $N \approx 60 \ (50 \lesssim N \lesssim 70)$ is about 13. Therefore, in a computationally feasible system, the chains with a degree of polymerization $N \approx 60$ have a higher probability of exchange with chains of similar degree of

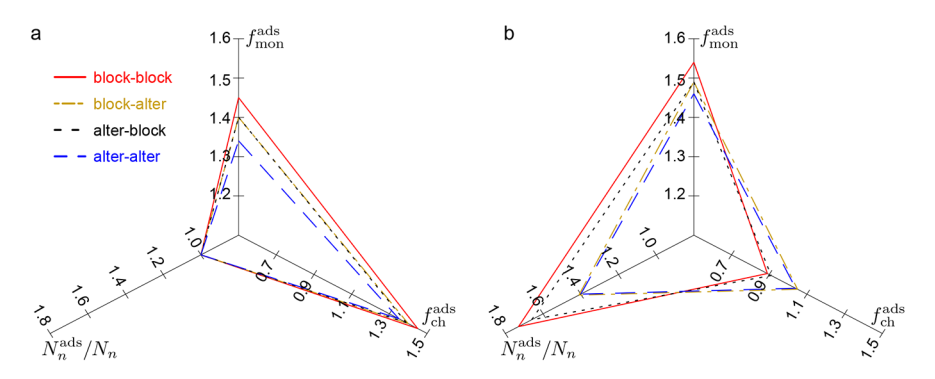


Figure 9. Radar plots displaying the fraction of adsorbed monomers (f_{ads}^{non}) , the fraction of adsorbed chains (f_{ads}^{nl}) , and the normalized number-averaged molecular weight (N_n^{nds}/N_n) for the block-block, block-alter, alter-block, and alter-alter architectures at $n_{\text{pa}}/n_{\text{pc}} = 4.7$. (a) D = 1.0 and (b) D = 1.5. The corresponding data and their error bars are tabulated in Table S3.

polymerization compared with chains with a degree of polymerization $N \approx 110$. (ii) The adsorption of longer chains is strong, whereupon a fraction of them adsorb quickly and the equilibrium state is one in which randomly chosen chains of this large length would spend the vast majority of their time adsorbed to the interface in a hypothetical infinitely long MD simulation. We return to a more detailed investigation into adsorption—desorption equilibrium later in the context of a bidisperse system to show that the latter simulations produce frequent chain exchange between polyanions with the same value of N when there are many such chains in the simulation.

Although the probability distribution of the degree of polymerizations of the adsorbed chains for the alter-alter case (Figure 8b) is qualitatively similar to the probability distribution of the degree of polymerizations of adsorbed chains for the block-block case (Figure 8a), the number of chains having $p_{ads} = 1$ or $p_{ads} = 0$ is smaller for alter—alter case compared to the block-block case. To explain these quantitative differences, we note that for monodisperse systems the adsorption free energy of polyanions in an alter-alter system is higher (weaker adsorption strength) compared to the block-block system. 21 The polyanion chains in an alter-alter system are likely to be in a weaker adsorption-desorption equilibrium with the brush chains compared to the blockblock system. While a detailed calculation of the average free energy of polydisperse chains could provide insights into this question, such a work is outside the scope of the current article.

While our primary focus is on the limiting cases of block block and alter-alter, it is illuminating to also consider the cases of mixed charge sequence, viz., the block-alter case (grafted chains in block charge sequence architecture and bulk chains in alternating charge sequence architecture) and the alter-block case (grafted chains in alternating charge sequence architecture and bulk chains with block charge sequence architecture). Figures 9a and 9b display radar plots for the fraction of adsorbed monomers (f_{ads}^{mon}), the fraction of adsorbed chains (f_{ads}^{ch}) , and the normalized number-averaged molecular weight $(N_n^{\rm ads}/N_n)$ for all the four different sequences at $n_{\rm pa}/n_{\rm pc}$ = 4.7 for D = 1.0 and D = 1.5, respectively. Within error bars, $f_{\text{ads}}^{\text{mon}}$, $f_{\text{ads}}^{\text{ch}}$ and N_n^{ads}/N_n for the block—alter and alter—block cases lie in between that of the block-block and the alter-alter sequences for both D = 1.0 and D = 1.5. In addition, the fraction of adsorbed monomers for D = 1.5 is higher compared to that for D = 1.0 irrespective of the charge sequence. For polydisperse cases (D = 1.5), the normalized fraction of adsorbed chains $(f_{\rm ads}^{\rm ch})$ and the normalized number-averaged molecular weights $(N_n^{\rm ads}/N_n)$ for the block—alter case are very similar to that of the alter—alter case, and that for the alter—block case is very similar to that of the block—block case. This result suggests that the adsorption is influenced by the charge sequence on the grafted polymers for polydisperse systems and that our analysis of block—block and alter—alter systems represents the two limiting cases.

DISCUSSION

The trends for adsorption as a function of degree of polymerization in Figure 8 can be understood in the context of a relatively simple model. Let c_N denote the number of polyanions of length N ("N-mers") per unit volume in the solution, and let Γ_N denote the number concentration of adsorbed chains of length N per unit area. We assume that the free energy gained by adding an adsorbed chain to the brush is proportional to the degree of polymerization N and that the chemical potential of a chain within the brush thus contains a contribution linear in N. This suggests that equating chemical potentials in the brush and solution leads to an equation of the form

$$k_{\rm B}T \ln(c_{\rm N}/c^{\circ}) = -EN + k_{\rm B}T \ln(\Gamma_{\rm N}/L_ac^{\circ})$$
 (1)

where c° is a standard concentration, L_a is a characteristic thickness for the adsorbed layer, $k_{\rm B}$ is Boltzmann's constant, T is temperature, and E is a binding free energy per monomer. Solving for Γ_N yields

$$\Gamma_N = L_a c_N e^{\beta EN} \tag{2}$$

where $\beta=1/(k_{\rm B}T)$. The binding free energy E is a quantity that depends on the state of the brush, which may arise from a combination of a decrease in electrostatic free energy per monomer when a polyanion is incorporated into the brush and an increase in counterion entropy when adsorption is accompanied by release of counterions from the brush. The key physical assumption of the theory is simply that, for a given state of the brush and a given sequence type (alternating or block), the contributions to μ_N arising from these physical effects increase linearly with the number of charged monomers (or total number of monomers) in an adsorbed chain.

Now consider a closed system in which M_N denotes the total number N-mers, and let p_N denote the fraction of adsorbed N-mers. If V is the volume of the bulk solution and A the interfacial area, then $\Gamma_N = M_N p_N / A$ and $c_N = M_N (1 - p_N) / V$. Using the latter in eq 2 yields

$$\frac{p_N}{A} = \frac{1 - p_N}{V} L_a e^{\beta EN} \tag{3}$$

which can be written in the form

$$\frac{p_N}{1 - p_N} = h e^{\beta E N} \tag{4}$$

in which the dimensionless quantity $h \equiv L_a A/V$ should be comparable to the fraction of the simulation unit cell occupied by the brush. Solving for p_N yields

$$p_{N} = \frac{he^{\beta EN}}{1 + he^{\beta EN}} \tag{5}$$

which is the model prediction for the functional form of the data in Figure 8.

The form of eq 4 suggests that the model parameters h and βE can be extracted from the data in Figure 8 by linear regression. To accomplish this task, we first removed all data with $p_{\rm ads} < 0.0001$ or $p_{\rm ads} > 0.9999$ to avoid singularities in the semilogarithmic plot and then fit the data up to a value $N_{\rm max}$ below which the data appeared to be linear. Figure 10a

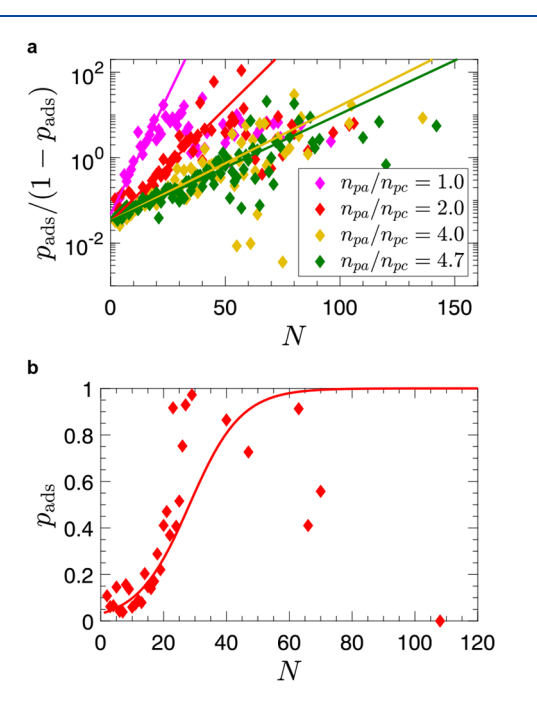


Figure 10. Results from the model for the probability of adsorption as a function of degree of polymerization. (a) Linear regression to eq 4 for the block—block case. The companion plot for the alter—alter case is provided in Figure S6. (b) Comparison of eq 5 with the linear regression coefficients in Table 1 and the data in Figure 8a for the block—block case for $n_{\rm pa}/n_{\rm pc}=2.0$. The plots for other cases are provided in Figures S7 and S8.

illustrates the result of this procedure for the block—block case using the $N_{\rm max}$ values in Table 1; the companion data for the alter—alter case are in Figure S6. To convert h into a form that allows easy comparison to the brush heights in, for example, Figure 2, note that the volume of the bulk solution is $V = (L_z - L_a)A$, whereupon $h = L_a/(L_z - L_a)$ or, equivalently, $L_a/L_z = h/(1+h)$ where $L_z = 120\sigma$ (see the Supporting Information). This fitting procedure, which only uses the sharply rising portion of the data in Figure 8, provides a satisfactory description of the entire data set in the panels of Figure 8 when

Table 1. Results of Linear Regression to the Data in Figure 8 Using Eq 4^a

		block-block		alter—alter	
$n_{\rm pa}/n_{\rm pc}$	$N_{ m max}$	L_a/L_z	βE	L_a/L_z	βΕ
1.0	25	0.045	0.26	0.053	0.19
2.0	40	0.031	0.12	0.064	0.075
4.0	80	0.032	0.062	0.078	0.038
4.7	80	0.032	0.058	0.103	0.023

"The value $N_{\rm max}$ is the upper bound used for linear regression. To compare the brush height with the data in Table S2, note that $L_z=120\sigma$.

plotted by using the form of eq 5. Figure 10b shows one example, and all of the cases are provided in Figures S7 and S8.

Three features emerge from the fitting data reported in Table 1. First, the values of the effective brush height L_a obtained from the regression to the theory are comparable to but somewhat lower than other measures of the height brush as shown in Figure 2, Figure S2, and Table S2. Such a quantitative difference is unsurprising given the simplicity of the model. Second, the marginal binding free energy per monomer E decreases with increasing number of polyanions over the range $n_{\rm pa}/n_{\rm pc} \geq 1.0$ considered here. The stronger adsorption at lower values of $n_{\rm pa}/n_{\rm pc}$ may reflect in part a free energy gain associated with the release of counterions upon adsorption of a polyanion, which dominates the adsorption free energy for n_{pa}/n_{pc} < 1 and may also occur to a lesser extent for values of $n_{\rm pa}/n_{\rm pc}$ slightly greater than unity. Third, for a given value of n_{pa}/n_{pc} , the binding free energy E is significantly larger for the block-block system than the alter-alter system. This observation, extracted from the N-dependence of the adsorption probability, is consistent with the larger number of monomers adsorbed for the block-block case in Figure 4 and presumably arises from the existence of a larger electrostatic correlation energy for the block-block case.

Overall, the most salient aspect of polydispersity is the presence of long chains in the mixture. The impact of these longer chains in the polydisperse system, in particular for the block—block architecture, is evident in the longer neutral tails sticking out of the brush (Figure 3a), the increase in the number of adsorbed monomers (Figure 4), the reduction in the total number of chains adsorbed (Figure 6), an increase in the average degree of polymerization of adsorbed chains (Figure 7), and the sigmoidal shape of the probability of adsorbing a chain of a given degree of polymerization (Figure 8). We attribute the preferential binding of the longer chains to the favorable translational entropy; binding a chain of size 2N to the brush costs less translational entropy than binding two chains of size N.

To probe the influence of the degree of polymerization distribution on the adsorption of polydisperse polyelectrolytes idea in a more straightforward, but less experimentally relevant, manner, we also simulated a simple bidisperse model. To this end, we constructed bidisperse blends of equal number polymer chains with high degree of polymerization (N=52) and low degree of polymerization (N=8). To identify the distribution of the adsorbed chains, we calculate $\phi_{\rm ads}$ defined as the ratio of fraction of chains adsorbed with N=52 to that with N=8. Figure 11 displays $\phi_{\rm ads}$ (yellow bar) for the blockblock and alter—alter cases with $n_{\rm pa}=150$ ($n_{\rm pa}/n_{\rm pc}=4.7$). For both the cases, $\phi_{\rm ads}$ is greater than 1, showing that the likelihood of adsorption of the high degree of polymerization

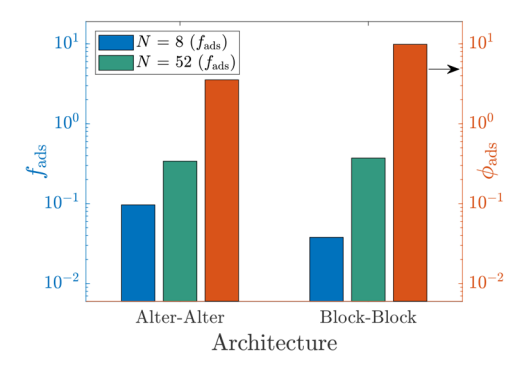


Figure 11. Comparison between the adsorbed fraction of bulk chains and the total number of bulk chains present in the simulation with the corresponding degree of polymerization in a bidisperse system for two different charge sequences. The red bar shows the ratio ($\phi_{\rm ads}$) between the fraction of chains adsorbed for N=52 (green bar) and N=8 (blue bar). The arrow mark shows the axis corresponding to the ratio ($\phi_{\rm ads}$). Results are averaged four independent simulations with $n_{\rm pa}=150$ and the polyanions modeled as a blend comprising equal number of low and high degree of polymerization chains. The error bars are negligible and are tabulated in Table S4.

chains is more than that for the low degree of polymerization chains. In addition, the low-N chains adsorb more efficiently for the alter—alter case when compared to the block—block case (compare blue bars in Figure 11). Therefore, a larger fraction of the total number of chains needs to be adsorbed for charge neutralization within the brush region. These results mirror the distribution for adsorbing chains of size N (Figure 8) and the fraction of polymers adsorbed for a polydisperse system (Figure 7). These simulations of a bidisperse system also allow us to revisit the question of adsorption equilibrium in Figure 8, since we now have many chains in each of the two bins. The identity of the set of adsorbed (or desorbed) chains at any time instant in Figure S5 is distinct, showing that long length chains in the bulk and brush regions exchange, and hence the system is at adsorption equilibrium.

■ CONCLUSION AND OUTLOOK

In summary, our work unequivocally shows that even moderate polydispersity (D=1.5) impacts many features of the brush, with an increased effect for a block-block architecture relative to the alter-alter charge sequence. These results are rationalized based on the translational entropy gains for keeping low degree of polymerization chains in solution in a polydisperse system. These results should prove useful for interpreting experiments on polyelectrolyte adsorption in processes with significant polydispersity.

Previous experimental works on polyelectrolyte adsorption along with the theory and simulations on the adsorption of monodisperse polyelectrolytes have shown that the polymer—polymer, polymer—particle, and polymer—surface interactions are dependent on salt concentration, ^{37–39} salt valency, ^{40–42} and local dielectric inhomogeneities, ^{43–45} and it is reasonable to anticipate that similar changes in the electrostatics could impact the result obtained here. With increasing salt valency, salt ions can competitively adsorb with shorter polymers in a polydisperse system. Moreover, at higher salt concentrations, screening becomes stronger, and the effects of electrostatics become weaker, leading to polyanions collapsing onto the grafted chains. ³⁷ In addition, the adsorption efficacy of polyelectrolytes on charged surfaces at high salt concentrations

was observed to depend on the charge sequence and chain length.³⁹ However, these trends are harder to predict for polydisperse systems as the reduction in enthalpic (electrostatics) contribution on adsorption becomes weaker and may become comparable to loss in entropic contributions (after adsorption) for longer adsorbed chains at high salt concentration. Finally, the effects of dielectric contrast may become predominant at polymer—polymer interfaces of longer chains since these effects become important for higher local polymer concentrations.⁴⁴ Understanding the effects of salt concentration, salt valency and dielectric contrast are avenues for interesting future works.

ASSOCIATED CONTENT

Supporting Information

The Supporting Information is available free of charge at https://pubs.acs.org/doi/10.1021/acs.macromol.1c02623.

Description of system setup; simulation technique; quantification measures; Figures S1–S8 and Tables S1–S4 (PDF)

AUTHOR INFORMATION

Corresponding Author

Kevin D. Dorfman – Department of Chemical Engineering and Materials Science, University of Minnesota, Twin Cities, Minneapolis, Minnesota 55455, United States; oorcid.org/0000-0003-0065-5157; Email: dorfman@umn.edu

Authors

Vaidyanathan Sethuraman – Department of Chemical Engineering and Materials Science, University of Minnesota, Twin Cities, Minneapolis, Minnesota 55455, United States

David Zheng — Department of Chemical Engineering and Materials Science, University of Minnesota, Twin Cities, Minneapolis, Minnesota SS4SS, United States

David C. Morse — Department of Chemical Engineering and Materials Science, University of Minnesota, Twin Cities, Minneapolis, Minnesota 55455, United States; orcid.org/ 0000-0002-1033-8641

Complete contact information is available at: https://pubs.acs.org/10.1021/acs.macromol.1c02623

Notes

The authors declare no competing financial interest. LAMMPS and analysis codes used in this article are available at https://github.com/vaidyanathanms/polydisperse_PE.git. Data for figures and restart files are available at https://doi.org/10.13020/RBJQ-NN61.

ACKNOWLEDGMENTS

This work was supported primarily by the National Science Foundation through the University of Minnesota Materials Science Research and Engineering Center under Awards DMR-1420013 and DMR-2011401. The authors acknowledge the Minnesota Supercomputing Institute (MSI) at the University of Minnesota for providing resources that contributed to the research results reported within this paper.

REFERENCES

(1) Overbeek, J. T. G.; Voorn, M. J. Phase separation in polyelectrolyte solutions: Theory of complex coacervation. *J. Cell. Physiol.* **1957**, 49, 7–26.

- (2) Muthukumar, M. Theory of counter-ion condensation on flexible polyelectrolytes: Adsorption mechanism. *J. Chem. Phys.* **2004**, *120*, 9343–9350.
- (3) Sing, C. E.; Perry, S. L. Recent progress in the science of complex coacervation. *Soft Matter* **2020**, *16*, 2885–2914.
- (4) Muthukumar, M. 50th Anniversary Perspective: A Perspective on Polyelectrolyte Solutions. *Macromolecules* **2017**, *50*, 9528–9560.
- (5) Perry, S. L.; Sing, C. E. 100th Anniversary of Macromolecular Science Viewpoint: Opportunities in the Physics of Sequence-Defined Polymers. *ACS Macro Lett.* **2020**, *9*, 216–225.
- (6) Pak, C. W.; Kosno, M.; Holehouse, A. S.; Padrick, S. B.; Mittal, A.; Ali, R.; Yunus, A. A.; Liu, D. R.; Pappu, R. V.; Rosen, M. K. Sequence Determinants of Intracellular Phase Separation by Complex Coacervation of a Disordered Protein. *Mol. Cell* **2016**, *63*, 72–85.
- (7) Carlsson, F.; Linse, P.; Malmsten, M. Monte Carlo Simulations of Polyelectrolyte-Protein Complexation. *J. Phys. Chem. B* **2001**, *105*, 9040–9049.
- (8) Cooper, C. L.; Dubin, P. L.; Kayitmazer, A. B.; Turksen, S. Polyelectrolyte—protein complexes. *Curr. Opin. Colloid Interface Sci.* **2005**, *10*, 52–78.
- (9) Antonov, M.; Mazzawi, M.; Dubin, P. L. Entering and Exiting the Protein-Polyelectrolyte Coacervate Phase via Nonmonotonic Salt Dependence of Critical Conditions. *Biomacromolecules* **2010**, *11*, 51–59.
- (10) Das, R. K.; Pappu, R. V. Conformations of intrinsically disordered proteins are influenced by linear sequence distributions of oppositely charged residues. *Proc. Natl. Acad. Sci. U. S. A.* **2013**, *110*, 13392–13397.
- (11) Kayitmazer, A. B.; Seeman, D.; Minsky, B. B.; Dubin, P. L.; Xu, Y. Protein-polyelectrolyte interactions. *Soft Matter* **2013**, *9*, 2553–2583.
- (12) Decher, G. Fuzzy Nanoassemblies: Toward Layered Polymeric Multicomposites. *Science* **1997**, 277, 1232–1237.
- (13) Decher, G. Multilayer Thin Films; John Wiley & Sons, Ltd.: 2012; Chapter 1, pp 1-21.
- (14) Hammond, P. T. Form and Function in Multilayer Assembly: New Applications at the Nanoscale. *Adv. Mater.* **2004**, *16*, 1271–1293.
- (15) Ai, H.; Jones, S. A.; Lvov, Y. M. Biomedical applications of electrostatic layer-by-layer nano-assembly of polymers, enzymes, and nanoparticles. *Cell Biochem. Biophys.* **2003**, *39*, 23.
- (16) Ko, Y. H.; Kim, Y. H.; Park, J.; Nam, K. T.; Park, J. H.; Yoo, P. J. Electric-Field-Assisted Layer-by-Layer Assembly of Weakly Charged Polyelectrolyte Multilayers. *Macromolecules* **2011**, *44*, 2866–2872.
- (17) Talingting, M. R.; Ma, Y.; Simmons, C.; Webber, S. E. Adsorption of Cationic Polymer Micelles on Polyelectrolyte-Modified Surfaces. *Langmuir* **2000**, *16*, 862–865.
- (18) Tan, Z.; Jiang, Y.; Zhang, W.; Karls, L.; Lodge, T. P.; Reineke, T. M. Polycation Architecture and Assembly Direct Successful Gene Delivery: Micelleplexes Outperform Polyplexes via Optimal DNA Packaging. *J. Am. Chem. Soc.* **2019**, *141*, 15804–15817.
- (19) Chang, L.-W.; Lytle, T. K.; Radhakrishna, M.; Madinya, J. J.; Vélez, J.; Sing, C. E.; Perry, S. L. Sequence and entropy-based control of complex coacervates. *Nat. Commun.* **2017**, *8*, 1273.
- (20) Laaser, J. E.; McGovern, M.; Jiang, Y.; Lohmann, E.; Reineke, T. M.; Morse, D. C.; Dorfman, K. D.; Lodge, T. P. Equilibration of Micelle-Polyelectrolyte Complexes: Mechanistic Differences between Static and Annealed Charge Distributions. *J. Phys. Chem. B* **2017**, *121*, 4631–4641.
- (21) Sethuraman, V.; McGovern, M.; Morse, D. C.; Dorfman, K. D. Influence of charge sequence on the adsorption of polyelectrolytes to oppositely-charged polyelectrolyte brushes. *Soft Matter* **2019**, *15*, 5431–5442.
- (22) Lynd, N. A.; Hillmyer, M. A.; Matsen, M. W. Theory of Polydisperse Block Copolymer Melts: Beyond the Schulz-Zimm Distribution. *Macromolecules* **2008**, *41*, 4531–4533.
- (23) Hartig, S. M.; Greene, R. R.; Dikov, M. M.; Prokop, A.; Davidson, J. M. Multifunctional nanoparticulate polyelectrolyte complexes. *Pharm. Res.* **2007**, *24*, 2353–2369.

- (24) Cordeiro, T. N.; Chen, P.-c.; De Biasio, A.; Sibille, N.; Blanco, F. J.; Hub, J. S.; Crehuet, R.; Bernadó, P. Disentangling polydispersity in the PCNA-p15PAF complex, a disordered, transient and multivalent macromolecular assembly. *Nucleic Acids Res.* **2017**, *45*, 1501–1515
- (25) Yu, J.; Jackson, N. E.; Xu, X.; Brettmann, B. K.; Ruths, M.; de Pablo, J. J.; Tirrell, M. Multivalent ions induce lateral structural inhomogeneities in polyelectrolyte brushes. *Sci. Adv.* **2017**, 3, eaa01497.
- (26) Zhang, H.; Rühe, J. Polyelectrolyte Multilayers on Weak Polyelectrolyte Brushes. *Macromol. Rapid Commun.* **2003**, *24*, 576–579.
- (27) Claesson, P. M.; Makuska, R.; Varga, I.; Meszaros, R.; Titmuss, S.; Linse, P.; Pedersen, J. S.; Stubenrauch, C. Bottle-brush polymers: Adsorption at surfaces and interactions with surfactants. *Adv. Colloid Interface Sci.* **2010**, *155*, 50–57.
- (28) Aguilera-Granja, F.; Kikuchi, R. Polymer statistics: IV. Simulation of adsorption of polymers and polyelectrolytes on surfaces. *Physica A* **1992**, *189*, 108–126.
- (29) Okrugin, B. M.; Richter, R. P.; Leermakers, F. A. M.; Neelov, I. M.; Borisov, O. V.; Zhulina, E. B. Structure and properties of polydisperse polyelectrolyte brushes studied by self-consistent field theory. *Soft Matter* **2018**, *14*, 6230–6242.
- (30) Zimm, B. H. Apparatus and Methods for Measurement and Interpretation of the Angular Variation of Light Scattering; Preliminary Results on Polystyrene Solutions. *J. Chem. Phys.* **1948**, *16*, 1099–1116.
- (31) Schulz, G. V. Über die Kinetik der Kettenpolymerisationen. V. Zeitschrift für Physikalische Chemie 1939, 43B, 25–46.
- (32) Plimpton, S. Fast Parallel Algorithms for Short-Range Molecular Dynamics. *J. Comput. Phys.* **1995**, *117*, 1–19.
- (33) Dobrynin, A. V.; Rubinstein, M. Theory of polyelectrolytes in solutions and at surfaces. *Prog. Polym. Sci.* **2005**, *30*, 1049–1118.
- (34) Nguyen, T. T.; Shklovskii, B. I. Model of Inversion of DNA Charge by a Positive Polymer: Fractionalization of the Polymer Charge. *Phys. Rev. Lett.* **2002**, *89*, 018101.
- (35) Ou, Z.; Muthukumar, M. Entropy and enthalpy of polyelectrolyte complexation: Langevin dynamics simulations. *J. Chem. Phys.* **2006**, *124*, 154902.
- (36) Cao, Q.; Zuo, C.; Li, L. Electrostatic binding of oppositely charged surfactants to spherical polyelectrolyte brushes. *Phys. Chem. Phys.* **2011**, *13*, 9706–9715.
- (37) Stoll, S.; Chodanowski, P. Polyelectrolyte Adsorption on an Oppositely Charged Spherical Particle. Chain Rigidity Effects. *Macromolecules* **2002**, *35*, 9556–9562.
- (38) Smith, A. M.; Lee, A. A.; Perkin, S. The Electrostatic Screening Length in Concentrated Electrolytes Increases with Concentration. *J. Chem. Phys. Lett.* **2016**, *7*, 2157–2163.
- (39) Chang, Q.; Jiang, J. Sequence Effects on the Salt-Enhancement Behavior of Polyelectrolytes Adsorption. *Macromolecules* **2022**, *55*, 897–905.
- (40) Kundagrami, A.; Muthukumar, M. Theory of competitive counterion adsorption on flexible polyelectrolytes: Divalent salts. *J. Chem. Phys.* **2008**, *128*, 244901.
- (41) Zhulina, E. B.; Borisov, O. V.; Birshtein, T. M. Polyelectrolyte Brush Interaction with Multivalent Ions. *Macromolecules* **1999**, *32*, 8189–8196.
- (42) Wang, L.; Liang, H.; Wu, J. Electrostatic origins of polyelectrolyte adsorption: Theory and Monte Carlo simulations. *J. Chem. Phys.* **2010**, *133*, 044906.
- (43) Nakamura, I.; Wang, Z.-G. Effects of dielectric inhomogeneity in polyelectrolyte solutions. *Soft Matter* **2013**, *9*, 5686–5690.
- (44) Pryamitsyn, V.; Ganesan, V. Pair interactions in polyelectrolytenanoparticle systems: Influence of dielectric inhomogeneities and the partial dissociation of polymers and nanoparticles. *J. Chem. Phys.* **2015**, *143*, 164904.
- (45) Samanta, R.; Ganesan, V. Influence of dielectric inhomogeneities on the structure of charged nanoparticles in neutral polymer solutions. *Soft Matter* **2018**, *14*, 3748–3759.